

Article

Design of Distributed Interval Observers for Multiple Euler–Lagrange Systems

Zhihang Yin ^{1,*} , Jun Huang ^{1,*}  and Thach Ngoc Dinh ^{2,*} 

¹ The School of Mechanical and Electrical Engineering, Soochow University, Suzhou 215325, China; 20215229080@stu.suda.edu.cn

² Conservatoire National des Arts et Métiers (CNAM), Cedric-Lab, 292, Rue Saint-Martin, CEDEX 03, 75141 Paris, France

* Correspondence: cauchyhot@163.com (J.H.); ngoc-thach.dinh@lecnam.net (T.N.D.)

Abstract: This paper investigates the problem of distributed interval estimation for multiple Euler–Lagrange systems. An interconnection topology is supposed to be strongly connected. To design distributed interval observers, the coordinate transformation method is employed. The construction of the distributed interval observer is given by the monotone system theory, and the stability is analyzed by the Lyapunov stability theory. Unlike the current works, each sub-interval observer has its own gain; in addition to this, additional observer gains are used to reduce the conservatism of design. The gains of all sub-interval observers are determined by both the monotone system theory and the Lyapunov stability theory. Finally, a simulation example verifies the feasibility of the presented distributed interval observers.

Keywords: distributed interval observers; multiple Euler–Lagrange systems; monotone system theory; Lyapunov stability theory

MSC: 37M25



Citation: Yin, Z.; Huang, J.; Dinh, T.N. Design of Distributed Interval Observers for Multiple Euler–Lagrange Systems. *Mathematics* **2023**, *11*, 1872. <https://doi.org/10.3390/math11081872>

Academic Editors: Fang Liu and Qianyi Liu

Received: 22 March 2023

Revised: 11 April 2023

Accepted: 12 April 2023

Published: 14 April 2023



Copyright: © 2023 by the authors. Licensee MDPI, Basel, Switzerland. This article is an open access article distributed under the terms and conditions of the Creative Commons Attribution (CC BY) license (<https://creativecommons.org/licenses/by/4.0/>).

1. Introduction

Euler–Lagrange systems (ELs) have been studied by a wide range of scholars as a common class of systems for describing many real mechanical models. In fact, some of the variables in a specific mechanical system are not directly available. Therefore, a number of scholars have addressed the observer design problem for ELs. A speed observer design method for general ELs was presented in [1]. The authors in [2] designed a nonlinear disturbance observer for ELs and realized the estimation of unknown disturbances. Ref. [3] used a sliding-mode disturbance observer for ELs to design a semi-global exponential controller. With the deepening of research and the development of multi-agent systems, scholars investigated the problem of the state estimation of multiple ELs (MELs) in recent years. In [4], the authors designed distributed observers (DOs) for a class of MELs without external disturbances. Ref. [5] studied the output-based tracking control problem for MELs, in which the authors designed a novel nonlinear DO. In [6], a DO-based fault-detection method for MELs was introduced, and a DO-based controller was also designed. In addition to this, the investigation on MELs with uncertainties had received considerable attention. Ref. [7] addressed the problem of leader-following consensus of uncertain MELs under switching network topology and proposed a DO design method to recover the states. Moreover, the distributed adaptive observers were designed for MELs with uncertainties in [8]. There are also other interesting works on MELs [9–12] herein.

As an effective estimation method, interval observers (IOs) can recover the upper and lower boundaries of uncertain systems. The concept of IOs was introduced in [13]. The IOs are further divided into centralized IOs (CIOs) and distributed IOs (DIOs). There are many studies on CIOs [14–21]. For continuous systems, an IO design method was introduced for

linear time-invariant systems with disturbances in [14]. The authors in [15] gave an effective design method of IO for time-varying systems. For discrete-time systems, [16] formulated a design framework of IO, and [17] investigated the IO design problem for time-varying discrete-time systems. In [18], the IO design method for discrete-time switched systems was studied. Over the past decade, the research of functional IO has also attracted the attention of some researchers [19–21]. On the other hand, the investigation on DIOs has also been reported by some works recently such as [22–24]. The authors of [22] presented an method to design DIOs, which was applied to fault detection for multi-agent systems. The authors of [23] considered the design method of DIOs for a class of linear time-invariant systems with uncertainties. Finally, The authors of [24] extended the DIOs design method to a class of fractional-order systems. The problem of estimation of MELs is always complicated due to the uncertainty contained in the system itself. Most of the existing works add constraints to achieve state estimation; however, this problem can be avoided if an interval estimation approach is used and state estimation can also be achieved. Therefore, it is necessary to design DIOs for MELs. To the authors’ best knowledge, there are few reports on DIOs for MELs.

Based on the above discussion, this paper studies the DIOs design problem of MELs. First of all, the coordinate transformation method must necessarily be introduced. Then, the framework of DIOs is constructed based on the monotone system theory. Additionally, the stability of DIO is guaranteed by Lyapunov stability theory. The rest of the paper is structured as follows. Section 2 gives the preliminaries, which include the graph theory and system model. Section 3 provides the DIO design method based on monotone system theory. In Section 4, a numerical example is used to show the validity of the presented design method of DIO. Finally, Section 5 is the conclusion of the paper.

Notation: For a matrix E , E^+ denotes $\max\{0, E\}$, $E^- = E^+ - E$. For a real symmetric matrix $O \in R^{n \times n}$, $O \succ 0$ ($O \prec 0$) indicates that O is positive (negative) definite, $He(O) = O^T + O$. \otimes represents the Kronecker product, and the $\text{diag}\{\cdot\}$ denotes a block diagonal matrix.

2. Preliminaries

2.1. Graph Theory

For a digraph G with N vertices, the adjacency matrix $\mathcal{A} \in R^{n \times n} = [a_{ij}]$ is given by $a_{ij} = 0$, if $(i, j) \in S$, where S is the set of edges, and $a_{ij} = 1$, otherwise. The length path from a vertex i to a vertex j is a sequence of $r + 1$ distinct vertices starting at i and ending at j , and consecutive vertices are adjacent to each other. A graph G is said to be connected if there is a path between any two vertices of the graph G . The Laplacian matrix \mathcal{L} of graph \mathcal{G} is defined as $\mathcal{L} := \mathcal{D} - \mathcal{A}$. \mathcal{D} is called the degree matrix of \mathcal{G} . For a connected graph, the Laplacian matrix has a single zero eigenvalue and the corresponding eigenvector is 1_N . Additionally, if G is connected then $0 = \lambda_1(G) \leq \lambda_2(G) \leq \dots \leq \lambda_N(G)$, where $\lambda_i(G)$ is the eigenvalue of \mathcal{L} .

Lemma 1 ([25]). Assume that \mathcal{G} is a strongly connected graph. Denote r_i ($i = 1, \dots, N$) as the left eigenvector with eigenvalue 0, and $R = \text{diag}\{r_1, \dots, r_N\}$; then, $R\mathcal{L} + \mathcal{L}^T R \geq 0$ holds.

Lemma 2 ([26]). If graph \mathcal{G} is strongly connected, the generalized algebraic connectivity of \mathcal{G} could be represented as $a(\mathcal{L}) = \min_{r^T x=0, x \neq 0} \frac{x^T (R\mathcal{L} + \mathcal{L}^T R)x}{2x^T R x}$. If the topology is balanced, the matrix $R = r_1 I_N$. Then, $a(\mathcal{L}) = \lambda_{\min}(\frac{He(\mathcal{L})}{2})$ holds.

2.2. System Model

In general, an ELS with second-order dynamics can be written as

$$M_i(q_i)\ddot{q}_i + C_i(q_i, \dot{q}_i)\dot{q}_i + G_i(q_i) = u_i, \tag{1}$$

where $q_i \in R^n$ is the vector of generalized coordinates, $M_i(q_i) \in R^{n \times n}$ represents the inertia matrix, $C(q_i, \dot{q}_i) \in R^{n \times n}$ denotes the vector of Coriolis and centripetal forces, $G(q) \in R^n$ is the gravity vector, and $u_i \in R^n$ stands for the vector of generalized control input forces. Next, we take the following transformations for system (1):

$$\begin{cases} \dot{x}_1 = x_2, \\ \dot{x}_2 = h(x_1)u + f(x_1, x_2), \end{cases} \tag{2}$$

where $x_{i1} = q_i$, $x_{i2} = \dot{q}_i$, $h(x_{i1}) = M(x_{i1})^{-1}$, $f(x_{i1}, x_{i2}) = -M(x_{i1})^{-1}(C(x_{i1}, x_{i2})x_{i2} + G(x_{i1}))$. The joint displacements are measurable; under the above state reconstruction, we can obtain the following equation:

$$\begin{cases} \dot{x}_i(t) = Ax_i(t) + Bu_i(t) + \phi_i(x_i(t)), \\ y_i(t) = Cx_i(t), \end{cases} \tag{3}$$

where $A = \begin{bmatrix} 0_{n \times n} & I_{n \times n} \\ 0_{n \times n} & 0_{n \times n} \end{bmatrix} \in R^{2n \times 2n}$, $B = \begin{bmatrix} 0_{n \times n} \\ h(x_{i1}) \end{bmatrix} \in R^{2n \times n}$, $C = [I_{n \times n} \ 0_{n \times n}] \in R^{n \times 2n}$, and $\phi_i(x_i(t)) = \begin{bmatrix} 0_{n \times 1} \\ f(x_{i1}, x_{i2}) \end{bmatrix} \in R^{2n}$.

Lemma 3 ([27]). *If $\phi(x_i)$ is a Lipschitz function that is globally differentiable, then there are two increasing Lipschitz functions $f(x_i)$ and $g(x_i)$ such that*

$$\phi(x_i) = f(x_i) - g(x_i). \tag{4}$$

Lemma 4 ([27]). *For the function $\phi(x_i)$ in Lemma 3, a global Lipschitz function $\bar{\phi}(x_{ia}, x_{ib})$ exists such that:*

- ★ $\bar{\phi}(x_i, x_i) = \phi(x_i)$,
- ★ $\frac{\partial \bar{\phi}}{\partial x_{ia}} \geq 0$, and $\frac{\partial \bar{\phi}}{\partial x_{ib}} \leq 0$.

The above lemmas can help us obtain the boundaries of nonlinear function $\phi(x_i, x_i)$:

$$x_i \leq x \leq \bar{x}_i \Rightarrow \bar{\phi}(x_i, \bar{x}_i) \leq \phi(x_i, x_i) \leq \bar{\phi}(\bar{x}_i, x_i). \tag{5}$$

Lemma 5 ([24]). *For $\phi(x_i)$, $\bar{\phi}(\bar{x}_i, x_i)$ and $\bar{\phi}(x_i, \bar{x}_i)$ defined in Lemma 4, matrices $F_i \in \{1, 2, 3, 4\}$ exist such that*

$$\begin{cases} \bar{\phi}(\bar{x}_i, x_i) - \phi(x_i) \leq F_1 \bar{e}_i + F_2 \underline{e}_i, \\ \phi(x_i) - \bar{\phi}(x_i, \bar{x}_i) \leq F_3 \bar{e}_i + F_4 \underline{e}_i, \end{cases} \tag{6}$$

where $\underline{e}_i = x_i - x_i$ and $\bar{e}_i = \bar{x}_i - x_i$.

Lemma 6 ([14]). *Given a constant matrix $A \in R^{m \times n}$ and a vector $\zeta \in R^{n \times 1}$, if $\zeta \in [\underline{\zeta}, \bar{\zeta}]$ holds, then*

$$A^+ \underline{\zeta} - A^- \bar{\zeta} \leq A \zeta \leq A^+ \bar{\zeta} - A^- \underline{\zeta}. \tag{7}$$

In order to obtain the main results, we need the following assumptions.

Assumption 1. *The nonlinear function $\phi_i(x_i(t))$ is considered as a global Lipschitz function.*

Assumption 2. *For every sub-system, the initial state of system (3) satisfies the following inequality:*

$$x_i(0) \leq x_i(0) \leq \bar{x}_i(0). \tag{8}$$

Assumption 3. The topology graph is considered to be balanced and strongly connected.

Assumption 4. Matrices L, M, \bar{Y} , and \underline{Y} exist such that Π is Metzler with

$$\Pi = \begin{bmatrix} \Psi + \bar{Y} & \bar{Y} \\ \underline{Y} & \Psi + \underline{Y} \end{bmatrix},$$

where $\Psi = \hat{A} - L\hat{C} - \gamma M(\mathcal{L} \otimes I_n)$.

Remark 1. The above assumptions have been commonly used and widely accepted in previous studies. Similar to [22], the topology graph is supposed to be balanced and strongly connected in this paper; based on this, we provide the following results.

3. Main Results

To design DIO for system (3), some preliminary preparations are needed. First, the equivalence transformation is performed for system matrix $A \in R^{n \times n}$. Using the linear transformation $z_i = Hx_i$, the system (3) becomes

$$\begin{cases} \dot{z}_i(t) = \bar{A}z_i(t) + \bar{B}u_i(t) + H\phi_i(H^{-1}z_i(t)), \\ y_i(t) = \bar{C}z_i(t), \end{cases} \tag{9}$$

where $\bar{A} = HAH^{-1}$, $\bar{B} = HB$, and $\bar{C} = CH^{-1}$.

Remark 2. In order to estimate the bounds of the nonlinear function $\phi_i(x)$, we define that

$$\begin{cases} \varphi_i(\bar{z}_i, z_i) = \phi_i(H_a^+ \bar{z}_i - H_a^- z_i, H_a^+ z_i - H_a^- \bar{z}_i), \\ \varphi_i(z_i, \bar{z}_i) = \phi_i(H_a^+ z_i - H_a^- \bar{z}_i, H_a^+ \bar{z}_i - H_a^- z_i), \end{cases} \tag{10}$$

where $\bar{z}_i(t)$ and $z_i(t)$ represent the estimated values of $z_i(t)$, and $H_a = H^{-1}$.

Under Lemma 6, the following inequality can be obtained:

$$\begin{aligned} \Phi_i(z_i, \bar{z}_i) &= H^+ \varphi_i(z_i, \bar{z}_i) - H^- \varphi_i(\bar{z}_i, z_i) \\ &\leq H\phi_i(H^{-1}z_i) \\ &\leq H^+ \varphi_i(\bar{z}_i, z_i) - H^- \varphi_i(z_i, \bar{z}_i) \\ &= \Phi_i(\bar{z}_i, z_i). \end{aligned}$$

Remark 3. After the transformation of the coordinates, the conclusion of Lemma 5 takes the following form:

$$\begin{cases} \Phi_i(\bar{z}_i, z_i) - H\phi_i(H^{-1}z_i) \leq N_1\bar{e}_i + N_2e_i, \\ H\phi_i(H^{-1}z_i) - \Phi_i(z_i, \bar{z}_i) \leq N_3\bar{e}_i + N_4e_i, \end{cases} \tag{11}$$

where $N_i = F_iH (i = 1, 2, 3, 4)$ are constant matrices.

To achieve $\underline{z} \leq z \leq \bar{z}$, the following DIOs for each sub-system are constructed:

$$\begin{cases} \dot{\bar{z}}_i(t) = \bar{A}\bar{z}_i(t) + \bar{B}u_i(t) + \Phi_i(\bar{z}_i, z_i) + L_i(y_i - \bar{C}\bar{z}_i(t)) + \bar{Y}_i(\bar{z}_i(t) - \underline{z}_i(t)) \\ \quad + \gamma M_i \sum_{j=0}^N a_{ij}(\bar{z}_j - \bar{z}_i), \\ \dot{\underline{z}}_i(t) = \bar{A}\underline{z}_i(t) + \bar{B}u_i(t) + \Phi_i(z_i, \bar{z}_i) + L_i(y_i - \bar{C}\underline{z}_i(t)) - \underline{Y}_i(\bar{z}_i(t) - \underline{z}_i(t)) \\ \quad + \gamma M_i \sum_{j=0}^N a_{ij}(\underline{z}_j - \underline{z}_i). \end{cases} \tag{12}$$

Then, the error system for i -th sub-system is obtained

$$\begin{cases} \dot{\bar{e}}_i(t) = \dot{\bar{z}}_i - \dot{z}_i \\ \quad = (\bar{A} - L_i \bar{C} - \gamma M_i \sum_{j=0}^N \mathcal{L}_{ij}) \bar{e}_i(t) + \Phi_i(\bar{z}_i, z_i) - H \phi_i(H^{-1} z_i(t)) + \bar{Y}_i(\bar{e}_i(t) - e_i(t)), \\ \dot{e}_i(t) = \dot{z}_i - \dot{\bar{z}}_i \\ \quad = (\bar{A} - L_i \bar{C} - \gamma M_i \sum_{j=0}^N \mathcal{L}_{ij}) e_i(t) + H \phi_i(H^{-1} z_i(t)) - \Phi_i(\bar{z}_i, z_i) + \underline{Y}_i(\bar{e}_i(t) - e_i(t)). \end{cases} \tag{13}$$

Under Assumption 3, the dynamics of the global system are expressed as

$$\begin{cases} \dot{z}(t) = \hat{A}z(t) + \hat{B}u(t) + \hat{\phi}(z(t)), \\ y(t) = \hat{C}z(t), \end{cases} \tag{14}$$

where $z = [z_1^T, \dots, z_N^T]^T$, $y = [y_1^T, \dots, y_N^T]^T$, $\hat{A} = \text{diag}\{\bar{A}, \dots, \bar{A}\}$, $\hat{B} = \text{diag}\{\bar{B}, \dots, \bar{B}\}$, $u = [u_1^T, \dots, u_N^T]^T$, $\hat{\phi} = [(H\phi_1)^T, \dots, (H\phi_N)^T]^T$, $\hat{C} = \text{diag}\{\bar{C}, \dots, \bar{C}\}$.

The dynamics of the global observer system are given by

$$\begin{cases} \dot{\bar{z}}(t) = \hat{A}\bar{z}(t) + \hat{B}u(t) + \bar{\Phi} + L(y - \hat{C}\bar{z}(t)) + \bar{Y}(\bar{z}(t) - z(t)) \\ \quad - \gamma M(\mathcal{L} \otimes I_n)\bar{z}(t), \\ \dot{z}(t) = \hat{A}z(t) + \hat{B}u(t) + \underline{\Phi} + L(y - \hat{C}z(t)) - \underline{Y}(\bar{z}(t) - z(t)) \\ \quad - \gamma M(\mathcal{L} \otimes I_n)z(t), \end{cases} \tag{15}$$

where $\bar{\Phi} = \begin{bmatrix} \Phi_1(\bar{z}_1, z_1) \\ \vdots \\ \Phi_N(\bar{z}_N, z_N) \end{bmatrix}$, $\underline{\Phi} = \begin{bmatrix} \Phi_1(z_1, \bar{z}_1) \\ \vdots \\ \Phi_N(z_N, \bar{z}_N) \end{bmatrix}$, $L = \begin{bmatrix} L_1 & & \\ & \ddots & \\ & & L_N \end{bmatrix}$, $\bar{Y} = \begin{bmatrix} \bar{Y}_1 & & \\ & \ddots & \\ & & \bar{Y}_N \end{bmatrix}$, $\underline{Y} = \begin{bmatrix} \underline{Y}_1 & & \\ & \ddots & \\ & & \underline{Y}_N \end{bmatrix}$.

Theorem 1. *If Assumptions 1–4 hold, the $\bar{z}(t)$ and $z(t)$ given in (15) satisfy $z(t) \leq z(t) \leq \bar{z}(t)$.*

Proof. The dynamics of the global error system are given by

$$\begin{cases} \dot{\bar{e}}(t) = \dot{\bar{z}}(t) - \dot{z}(t) \\ \quad = [\hat{A} - L\hat{C} - \gamma M(\mathcal{L} \otimes I_n)]\bar{e}(t) + \bar{\Phi} - \hat{\phi}(z(t)) + \bar{Y}(\bar{e}(t) - e(t)), \\ \dot{e}(t) = \dot{z}(t) - \dot{\bar{z}}(t) \\ \quad = [\hat{A} - L\hat{C} - \gamma M(\mathcal{L} \otimes I_n)]e(t) + \hat{\phi}(z(t)) - \underline{\Phi} + \underline{Y}(\bar{e}(t) - e(t)). \end{cases} \tag{16}$$

Define $\epsilon(t) = \begin{bmatrix} \bar{e}(t) \\ e(t) \end{bmatrix}$, then we can obtain the derivative of $\epsilon(t)$

$$\dot{\epsilon}(t) = \Pi\epsilon(t) + \check{\Phi}, \tag{17}$$

where

$$\Pi = \begin{bmatrix} \Psi + \bar{Y} & \bar{Y} \\ \underline{Y} & \Psi + \underline{Y} \end{bmatrix}, \check{\Phi} = \begin{bmatrix} \bar{\Phi} - \hat{\phi}(z(t)) \\ \hat{\phi}(z(t)) - \underline{\Phi} \end{bmatrix}. \tag{18}$$

The proof of the validity of (12) and (15) is equivalent to the proof of the non-negativity of the error system. From Lemma 4 and Remark 2, we have $\bar{\Phi} - \hat{\phi}(z(t)) \geq 0$ and $\hat{\phi}(z(t)) - \underline{\Phi} \geq 0$.

$\Phi \geq 0$. It is obvious that $\bar{e}(0) \geq 0$ and $\underline{e}(0) \geq 0$ from Assumption 2. By Assumption 4, we have Π is Metzler. Above all, considering the monotone system theory, $\epsilon(t) \geq 0$ holds, which implies $\underline{z}(t) \leq z(t) \leq \bar{z}(t)$ for all $t \geq 0$. Hence, the proof of Theorem 1 is completed.

After proving the boundedness of DIO, we proceed to design the observer gain $L_i, \bar{Y}_i, \underline{Y}_i$, and M_i to guarantee the stability of the DIO (15).

Theorem 2. Given a positive definite matrix $P = P^T$ and a constant $\tau > 0$, if a solution exists such that

$$\tilde{\Omega} = \begin{bmatrix} He(P\bar{A} - Q_i\bar{C} + PN_1 + \bar{W}_i) - 2\tau I_n & PN_2 - \bar{W}_i + N_3^T P + \underline{W}_i^T \\ N_2^T P - \bar{W}_i^T + PN_3 + \underline{W}_i & He(P\bar{A} - Q_i\bar{C} + PN_4 - \underline{W}_i) - 2\tau I_n \end{bmatrix} \leq 0, \tag{19}$$

$$\gamma > \frac{\tau}{a(\mathcal{L})},$$

where $L_i = P^{-1}Q_i, \bar{Y}_i = P^{-1}\bar{W}_i, \underline{Y}_i = P^{-1}\underline{W}_i$, and $M_i^{-1} = P$ are the observer gains, γ is the coupling strength, then the system (15) is a DIO of (14).

Proof. A Lyapunov function candidate can be defined as $V(t) = \sum_{i=0}^N r_i \bar{e}_i^T P \bar{e}_i + \sum_{i=0}^N r_i \underline{e}_i^T P \underline{e}_i$; then, the derivative of $V(t)$ can be written as \square

$$\begin{aligned} \dot{V}(t) &= \sum_{i=0}^N r_i (\Gamma \bar{e}_i + \bar{\chi}_i + \bar{Y}_i (\bar{e}_i - \underline{e}_i))^T P \bar{e}_i + \sum_{i=0}^N r_i (\Gamma \underline{e}_i + \underline{\chi}_i + \underline{Y}_i (\bar{e}_i - \underline{e}_i))^T P \underline{e}_i \\ &+ \sum_{i=0}^N r_i \bar{e}_i^T P (\Gamma \bar{e}_i + \bar{\chi}_i + \bar{Y}_i (\bar{e}_i - \underline{e}_i)) + \sum_{i=0}^N r_i \underline{e}_i^T P (\Gamma \underline{e}_i + \underline{\chi}_i + \underline{Y}_i (\bar{e}_i - \underline{e}_i)) \\ &\leq \sum_{i=0}^N r_i (\Gamma \bar{e}_i + N_1 \bar{e}_i + N_2 \underline{e}_i + \bar{Y}_i (\bar{e}_i - \underline{e}_i))^T P \bar{e}_i \\ &+ \sum_{i=0}^N r_i (\Gamma \underline{e}_i + N_3 \bar{e}_i + N_4 \underline{e}_i + \underline{Y}_i (\bar{e}_i - \underline{e}_i))^T P \underline{e}_i \\ &+ \sum_{i=0}^N r_i \bar{e}_i^T P (\Gamma \bar{e}_i + N_1 \bar{e}_i + N_2 \underline{e}_i + \bar{Y}_i (\bar{e}_i - \underline{e}_i)) \\ &+ \sum_{i=0}^N r_i \underline{e}_i^T P (\Gamma \underline{e}_i + N_3 \bar{e}_i + N_4 \underline{e}_i + \underline{Y}_i (\bar{e}_i - \underline{e}_i)) \tag{20} \\ &= ((R \otimes (\bar{A} - L_i \bar{C}) - \gamma R \mathcal{L} \otimes M_i) \bar{e} + R \otimes (N_1 + \bar{Y}_i) \bar{e} + R \otimes (N_2 - \bar{Y}_i) \underline{e})(I \otimes P) \bar{e} \\ &+ ((R \otimes (\bar{A} - L_i \bar{C}) - \gamma R \mathcal{L} \otimes M_i) \underline{e} + R \otimes (N_3 + \underline{Y}_i) \bar{e} + R \otimes (N_4 - \underline{Y}_i) \underline{e})(I \otimes P) \underline{e} \\ &+ \bar{e}^T (I \otimes P) ((R \otimes (\bar{A} - L_i \bar{C}) - \gamma R \mathcal{L} \otimes M_i) \bar{e} + R \otimes (N_1 + \bar{Y}_i) \bar{e} + R \otimes (N_2 - \bar{Y}_i) \underline{e}) \\ &+ \underline{e}^T (I \otimes P) ((R \otimes (\bar{A} - L_i \bar{C}) - \gamma R \mathcal{L} \otimes M_i) \underline{e} + R \otimes (N_3 + \underline{Y}_i) \bar{e} + R \otimes (N_4 - \underline{Y}_i) \underline{e}) \\ &= \bar{e}^T (R \otimes He(P\bar{A} - PL_i \bar{C} + P(N_1 + \bar{Y}_i)) - \gamma (R \mathcal{L} + \mathcal{L}^T R) \otimes PM) \bar{e} \\ &+ \bar{e}^T (R \otimes (P(N_2 - \bar{Y}_i) + (N_3 + \underline{Y}_i)^T P)) \underline{e} + \underline{e}^T (R \otimes ((N_2 - \bar{Y}_i)^T P + P(N_3 + \underline{Y}_i))) \bar{e} \\ &+ \underline{e}^T (R \otimes He(P\bar{A} - PL_i \bar{C} + P(N_4 - \underline{Y}_i)) - \gamma (R \mathcal{L} + \mathcal{L}^T R) \otimes PM) \underline{e}, \end{aligned}$$

where $\Gamma = \bar{A} - L_i \bar{C} - \gamma M_i \sum_{j=0}^N \mathcal{L}_{ij}, \bar{\chi}_i = \Phi_i(\bar{z}_i, z_i) - H\phi_i(H^{-1}z_i(t))$, and $\underline{\chi}_i = H\phi_i(H^{-1}z_i(t)) - \Phi_i(z_i, \bar{z}_i)$.

It follows from Lemma 2 that

$$2a(\mathcal{L})\bar{e}^T R \bar{e} \leq \bar{e}^T (R \mathcal{L} + \mathcal{L}^T R) \bar{e}, \tag{21}$$

$$2a(\mathcal{L})\underline{e}^T R \underline{e} \leq \underline{e}^T (R \mathcal{L} + \mathcal{L}^T R) \underline{e}. \tag{22}$$

Considering $M_i = P^{-1}$, (21) and (22), (20) can be written as

$$\begin{aligned} \dot{V}(t) \leq & \bar{e}^T (R \otimes He(P\bar{A} - PL_i\bar{C} + P(N_1 + \bar{Y}_i)) - 2\gamma a(\mathcal{L})R \otimes I_n) \bar{e} \\ & + \bar{e}^T (R \otimes (P(N_2 - \bar{Y}_i) + (N_3 + \underline{Y}_i)^T P)) \underline{e} + \underline{e}^T (R \otimes ((N_2 - \bar{Y}_i)^T P + P(N_3 + \underline{Y}_i))) \bar{e} \\ & + \underline{e}^T (R \otimes He(P\bar{A} - PL_i\bar{C} + P(N_4 - \underline{Y}_i)) - 2\gamma a(\mathcal{L})R \otimes I_n) \underline{e}. \end{aligned} \tag{23}$$

Noting that $\gamma > \frac{\tau}{a(\mathcal{L})}$, we have

$$\begin{aligned} \dot{V}(t) \leq & \bar{e}^T (R \otimes He(P\bar{A} - PL_i\bar{C} + P(N_1 + \bar{Y}_i)) - 2\tau R \otimes I_n) \bar{e} \\ & + \bar{e}^T (R \otimes (P(N_2 - \bar{Y}_i) + (N_3 + \underline{Y}_i)^T P)) \underline{e} + \underline{e}^T (R \otimes ((N_2 - \bar{Y}_i)^T P + (PN_3 + \underline{Y}_i))) \bar{e} \\ & + \underline{e}^T (R \otimes He(P\bar{A} - PL_i\bar{C} + P(N_4 - \underline{Y}_i)) - 2\tau R \otimes I_n) \underline{e} \\ = & \epsilon^T(t) R \otimes \Omega \epsilon(t), \end{aligned} \tag{24}$$

where $\epsilon(t) = [\bar{e}^T, \underline{e}^T]^T$, and

$$\Omega = \begin{bmatrix} He(P\bar{A} - PL_i\bar{C} + P(N_1 + \bar{Y}_i)) - 2\tau I_n & P(N_2 - \bar{Y}_i) + (N_3 + \underline{Y}_i)^T P \\ (N_2 - \bar{Y}_i)^T P + P(N_3 + \underline{Y}_i) & He(P\bar{A} - PL_i\bar{C} + P(N_4 - \underline{Y}_i)) - 2\tau I_n \end{bmatrix}. \tag{25}$$

Then, $\dot{V}(t) < 0$ and $\Omega \prec 0$ are equal, which shows that $\lim_{t \rightarrow \infty} \bar{e}(t) = 0$ and $\lim_{t \rightarrow \infty} \underline{e}(t) = 0$. The stability of DIO can be guaranteed.

Remark 4. To satisfy the LMI toolbox, $Q_i = PL_i, \bar{W}_i = P\bar{Y}_i, \underline{W}_i = P\underline{Y}_i$ are applied to Ω , which results in

$$\tilde{\Omega} = \begin{bmatrix} He(P\bar{A} - Q_i\bar{C} + PN_1 + \bar{W}_i) - 2\tau I_n & PN_2 - \bar{W}_i + N_3^T P + \underline{W}_i^T \\ N_2^T P - \bar{W}_i^T + PN_3 + \underline{W}_i & He(P\bar{A} - Q_i\bar{C} + PN_4 - \underline{W}_i) - 2\tau I_n \end{bmatrix}.$$

4. Simulation

In this section, a team of 2-DOF manipulator models with an directed graph is applied to validate the feasibility of the presented DIOs for ELSs. The example runs on a CPU Inter Core i7-10750H CPU with 2.59 GHZ and 8 GB of RAM; the main software used is MATLAB 2018a.

The parameters of the model can be referred to [12], and the description of the parameters is shown in Table 1. First of all, the matrix \mathcal{L} is

$$\mathcal{L} = \begin{bmatrix} 3 & -1 & -1 & -1 \\ -1 & 2 & -1 & 0 \\ -1 & -1 & 2 & 0 \\ -1 & 0 & 0 & 1 \end{bmatrix},$$

From Lemma 2, it follows that $\alpha(\mathcal{L}) = 1$. Then, we chose the coordinate transformation matrix as

$$H = \begin{bmatrix} 1 & 0 & 0 & 0 \\ 0 & 1 & 0 & 0 \\ -1 & 0 & 1 & 0 \\ 0 & -1 & 0 & 1 \end{bmatrix}.$$

By solving (19), the gain of the observer can be calculated.

$$\bar{W}_i = \begin{bmatrix} 1.7448 & 0 & 0.3703 & 0 \\ 0 & 1.7448 & 0 & 0.3703 \\ 0.3703 & 0 & 1.0920 & 0 \\ 0 & 0.3703 & 0 & 1.0920 \end{bmatrix}, \underline{W}_i = \begin{bmatrix} -1.7448 & 0 & -0.3703 & 0 \\ 0 & -1.7448 & 0 & -0.3703 \\ -0.3703 & 0 & -1.0920 & 0 \\ 0 & -0.3703 & 0 & -1.0920 \end{bmatrix},$$

$$Q = \begin{bmatrix} 5.3976 & 0 \\ 0 & 5.3976 \\ 3.0250 & 0 \\ 0 & 3.0250 \end{bmatrix}, M_i = \begin{bmatrix} 0.5235 & 0 & 0.0920 & 0 \\ 0 & 0.5235 & 0 & 0.0920 \\ 0.0920 & 0 & 0.8917 & 0 \\ 0 & 0.0920 & 0 & 0.8917 \end{bmatrix},$$

and

$$P = \begin{bmatrix} 1.9456 & 0 & -0.2008 & 0 \\ 0 & 1.9456 & 0 & -0.2008 \\ -0.2008 & 0 & 1.1422 & 0 \\ 0 & -0.2008 & 0 & 1.1422 \end{bmatrix}.$$

Noting Remark 4, we can obtain

$$\bar{Y}_i = \begin{bmatrix} 0.9474 & 0 & 0.2943 & 0 \\ 0 & 0.9474 & 0 & 0.2943 \\ 0.4908 & 0 & 1.0078 & 0 \\ 0 & 0.4908 & 0 & 1.0078 \end{bmatrix}, \underline{Y}_i = \begin{bmatrix} -0.9474 & 0 & -0.2943 & 0 \\ 0 & -0.9474 & 0 & -0.2943 \\ -0.4908 & 0 & -1.0078 & 0 \\ 0 & -0.4908 & 0 & -1.0078 \end{bmatrix},$$

$$L_i = \begin{bmatrix} 3.1040 & 0 \\ 0 & 3.1040 \\ 3.1941 & 0 \\ 0 & 3.1941 \end{bmatrix}.$$

The initial value is defined as $x(0) = [0 \ 5 \ 6 \ 4 \ 4 \ 1 \ 5 \ 6 \ 3 \ 4 \ 6 \ 1 \ 6 \ 4 \ 1 \ 5]^T$. The initial values of DIO are chosen as $\bar{x}(0) = [10 \ 10 \ 9 \ 7 \ 10 \ 10 \ 13 \ 9 \ 10 \ 10 \ 7 \ 13 \ 10 \ 10 \ 8 \ 10]^T$ and $\underline{x}(0) = [-4 \ -4 \ -4.5 \ -3.5 \ -4 \ -4 \ -5 \ -1 \ -4 \ -4 \ -4 \ -6 \ -4 \ -4 \ -1 \ -4]^T$, and γ is given as $\gamma = 3$.

Table 1. The descriptions of the parameters.

Parameter	Description ($i = 1, 2, 3, 4$)
q_i	The position of manipulator i
\dot{q}_i	The velocity of manipulator i
\ddot{q}_i	The acceleration of manipulator i
M_i	The inertia matrix of manipulator i
C_i	The vector of Coriolis and centrifugal force of manipulator i
G_i	The vector of Gravitational force of manipulator i
u_i	The control input of manipulator i

The simulation results are displayed in the figures below. It is worth noting that i in v_{ij} refers to the i -th manipulator and j represents the j -th state. Figures 1–4 depict the original state trajectory of velocity and the state trajectory of DIO at the two joints of the four manipulators, respectively. It can be seen that the boundaries of the DIO recover the state of the original system. Figures 5–8 show the errors in the DIO and the original system velocity for the four manipulators at the two joints, respectively. From the figures, we can see that the error between the original system and observer converge to a small bound, which means that the DIO is valid.

Remark 5. In the simulation, we first need to design a coordinate transformation matrix and then solve $\tilde{\Omega} < 0$ (25) by using the LMI toolbox, and the feasible solution is applied to the simulation model we have built. The complexity of the computation is reflected in solving the LMI, and the details are shown in Table 2.

Table 2. Complexity of the calculation.

Parameter	Description	Time
\bar{W}_i	Observer gain	0.436 s
W_i	Observer gain	0.436 s
Q	Observer gain	0.456 s
M_i	Weight matrix	0.318 s
P	Weight matrix	0.318 s
\bar{Y}_i	Observer gain	0.624 s
Y_i	Observer gain	0.624 s
L_i	Observer gain	0.624 s

It is worth noting that the parameters in Table 2 all need to be recalculated if the topology or the coordinate transformation matrix changes.

Remark 6. Compared with [22], MELs contain nonlinearities, which makes it more complicated to design the IO. That is, the design method proposed in the paper can also be applied to more general systems. Unlike [24], two observer gains \bar{Y}_i and Y_i are considered to make the sufficient condition less conservative while ensuring the existence of the interval observer. As shown in Table 3, the conditions obtained using the method in this article are solvable. However, using the method in [24], there is no solution.

Table 3. The solution under different τ [24].

Value of τ	Theorem 2	Theorem 2 in [24]
-100	✓	-

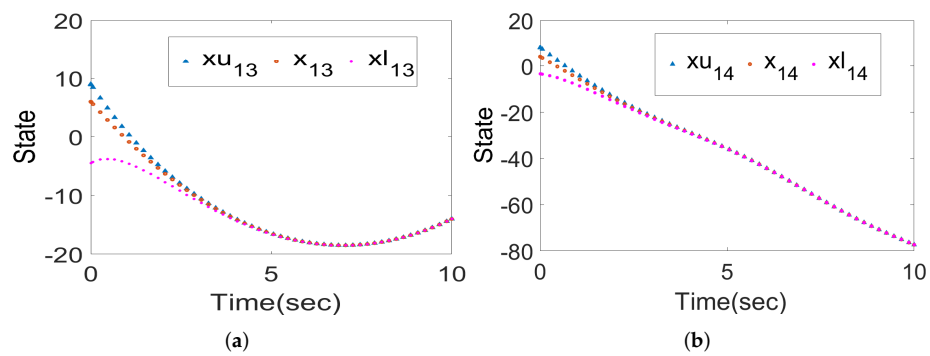


Figure 1. Evolutions of velocity of original system and DIO at the first joint (a) and second joint (b) of first manipulator.

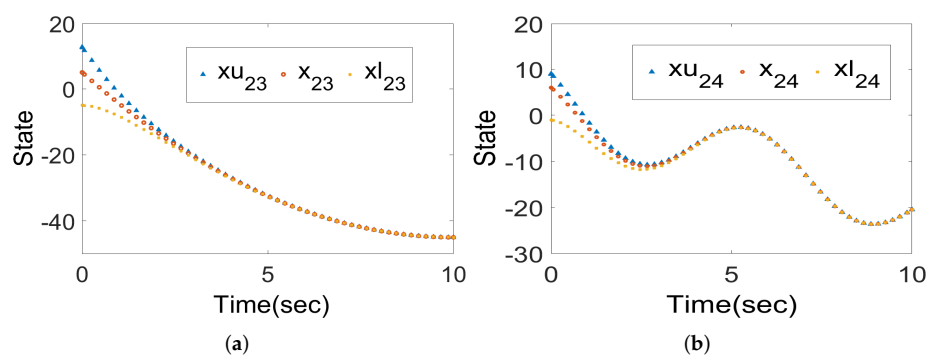


Figure 2. Evolutions of velocity of original system and DIO at the first joint (a) and second joint (b) of second manipulator.

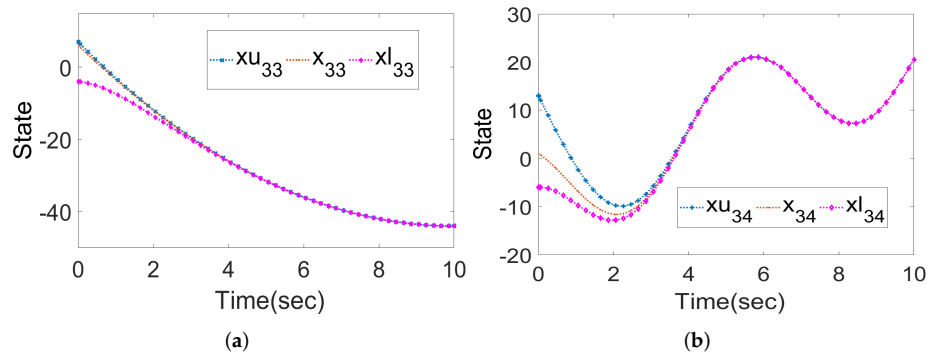


Figure 3. Evolutions of velocity of original system and DIO at the first joint (a) and second joint (b) of third manipulator.

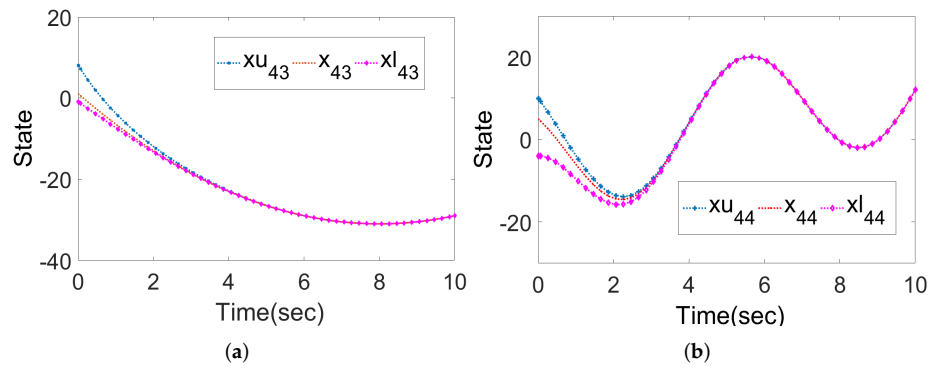


Figure 4. Evolutions of velocity of original system and DIO at the first joint (a) and second joint (b) of fourth manipulator.

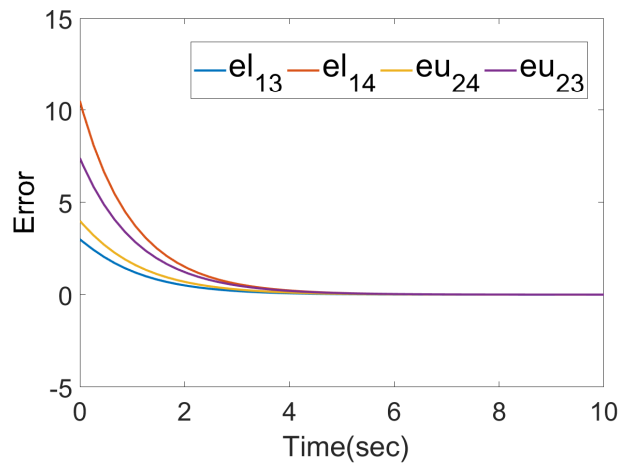


Figure 5. The error between the observer and the original system of the first manipulator.

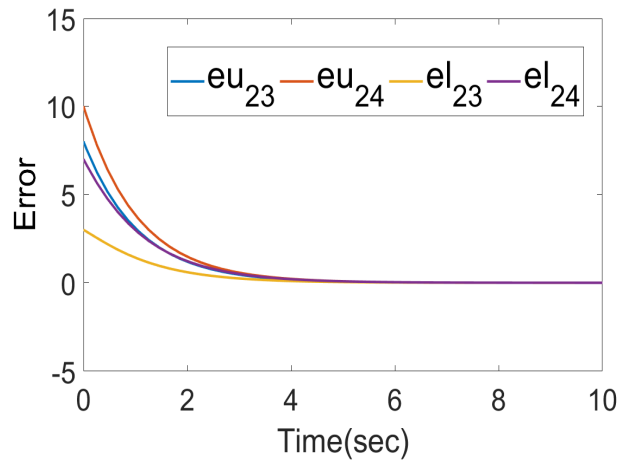


Figure 6. The error between the observer and the original system of the second manipulator.

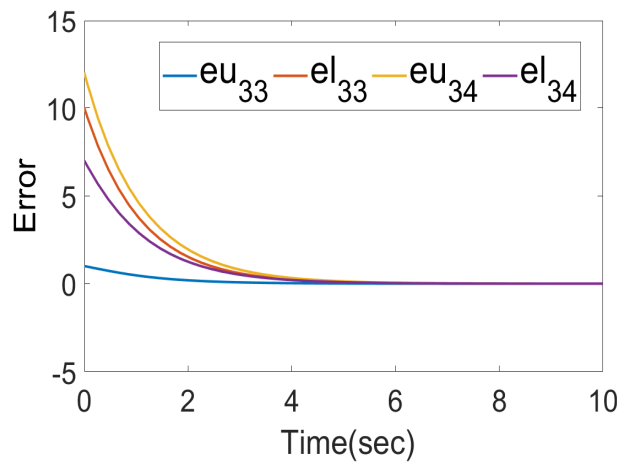


Figure 7. The error between the observer and the original system of the third manipulator.

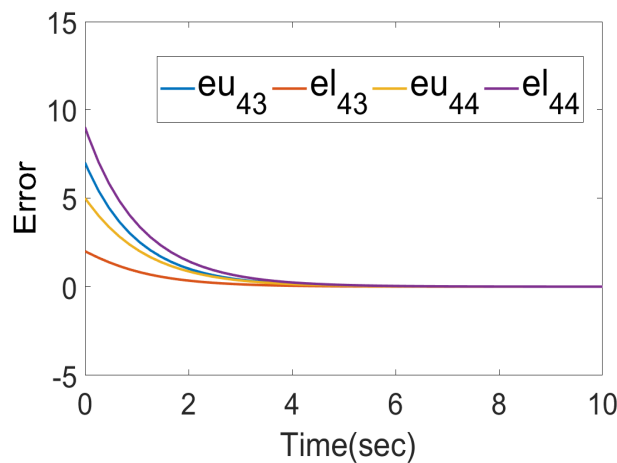


Figure 8. The error between the observer and the original system of the fourth manipulator.

5. Conclusions

In this paper, a DIO design method for MELs is studied. The design conditions are relaxed by using the coordinate transformation method. Two methods of designing observer gains are formulated under monotone system theory and Lyapunov stability theory. Meanwhile, the additional observer gains \tilde{Y} and \underline{Y} are introduced in DIO, which also provide more feasibility for the existence of the observer. Finally, an example is given

to verify the effectiveness of the presented DIO design method. In the future, we will try to relax the requirements of the topology graph and study the design of DIO-based controller algorithms.

Author Contributions: Conceptualization, Z.Y. and J.H.; Methodology, Z.Y., J.H. and T.N.D.; Validation, Z.Y., J.H. and T.N.D.; Writing—original draft, Z.Y.; Writing—review & editing, J.H. and T.N.D.; Supervision, J.H. All authors have read and agreed to the published version of the manuscript.

Funding: This research received no external funding.

Data Availability Statement: Not applicable.

Conflicts of Interest: The authors declare no conflict of interest.

References

1. Starnes, Ø.N.; Aamo, O.M.; Kaasa, G.O. A constructive speed observer design for general Euler–Lagrange systems. *Automatica* **2011**, *47*, 2233–2238. [[CrossRef](#)]
2. Mohammadi, A.; Marquez, H.J.; Tavakoli, M. Nonlinear disturbance observers: Design and applications to Euler–Lagrange systems. *IEEE Control Syst. Mag.* **2017**, *37*, 50–72.
3. Sun, T.; Cheng, L.; Wang, W.; Pan, Y. Semiglobal exponential control of Euler–Lagrange systems using a sliding-mode disturbance observer. *Automatica* **2020**, *112*, 108677. [[CrossRef](#)]
4. Starnes, Ø.N.; Aamo, O.M.; Kaasa, G.O. Global output feedback tracking control of Euler–Lagrange systems. *IFAC Proc. Vol.* **2011**, *44*, 215–220. [[CrossRef](#)]
5. Yang, Q.; Fang, H.; Mao, Y.; Huang, J. Distributed tracking for networked Euler–Lagrange systems without velocity measurements. *J. Syst. Eng. Electron.* **2014**, *25*, 671–680. [[CrossRef](#)]
6. Liu, L.; Shan, J. Distributed formation control of networked Euler–Lagrange systems with fault diagnosis. *J. Frankl. Inst.* **2015**, *352*, 952–973. [[CrossRef](#)]
7. Cai, H.; Huang, J. Leader-following consensus of multiple uncertain Euler–Lagrange systems under switching network topology. *Int. J. Gen. Syst.* **2014**, *43*, 294–304. [[CrossRef](#)]
8. Cai, H.; Huang, J. The leader-following consensus for multiple uncertain Euler–Lagrange systems with a distributed adaptive observer. In Proceedings of the 2015 IEEE 7th International Conference on Cybernetics and Intelligent Systems (CIS) and IEEE Conference on Robotics, Automation and Mechatronics (RAM), Siem Reap, Cambodia, 15–17 July 2015; pp. 218–223.
9. Cai, H.; Huang, J. The leader-following consensus for multiple uncertain Euler–Lagrange systems with an adaptive distributed observer. *IEEE Trans. Autom. Control* **2015**, *61*, 3152–3157. [[CrossRef](#)]
10. Wang, S.; Huang, J. Adaptive leader-following consensus for multiple Euler–Lagrange systems with an uncertain leader system. *IEEE Trans. Neural Netw. Learn. Syst.* **2018**, *30*, 2188–2196. [[CrossRef](#)]
11. Guo, X.; Wei, G.; Yao, M.; Zhang, P. Consensus Control for Multiple Euler–Lagrange Systems Based on High-Order Disturbance Observer: An Event-Triggered Approach. *IEEE/CAA J. Autom. Sin.* **2022**, *9*, 945–948. [[CrossRef](#)]
12. Sun, Y.; Dong, D.; Qin, H.; Wang, W. Distributed tracking control for multiple Euler–Lagrange systems with communication delays and input saturation. *ISA Trans.* **2020**, *96*, 245–254. [[CrossRef](#)] [[PubMed](#)]
13. Gouzé, J.L.; Rapaport, A.; Hadj-Sadok, M.Z. Interval observers for uncertain biological systems. *Ecol. Model.* **2000**, *133*, 45–56. [[CrossRef](#)]
14. Mazenc, F.; Bernard, O. Interval observers for linear time-invariant systems with disturbances. *Automatica* **2011**, *47*, 140–147. [[CrossRef](#)]
15. Thabet, R.E.H.; Raïssi, T.; Combastel, C.; Efimov, D.; Zolghadri, A. An effective method to interval observer design for time-varying systems. *Automatica* **2014**, *50*, 2677–2684. [[CrossRef](#)]
16. Mazenc, F.; Dinh, T.N.; Niculescu, S.I. Interval observers for discrete-time systems. *Int. J. Robust Nonlinear Control* **2014**, *24*, 2867–2890. [[CrossRef](#)]
17. Efimov, D.; Perruquetti, W.; Raïssi, T.; Zolghadri, A. Interval observers for time-varying discrete-time systems. *IEEE Trans. Autom. Control* **2013**, *58*, 3218–3224. [[CrossRef](#)]
18. Guo, S.; Zhu, F. Interval observer design for discrete-time switched system. *IFAC-PapersOnLine* **2017**, *50*, 5073–5078. [[CrossRef](#)]
19. Gu, D.K.; Liu, L.W.; Duan, G.R. Functional interval observer for the linear systems with disturbances. *IET Control Theory Appl.* **2018**, *12*, 2562–2568. [[CrossRef](#)]
20. Raïssi, T.; Videau, G.; Zolghadri, A. Interval observer design for consistency checks of nonlinear continuous-time systems. *Automatica* **2010**, *46*, 518–527. [[CrossRef](#)]
21. Huong, D.C. Design of functional interval observers for non-linear fractional-order systems. *Asian J. Control* **2020**, *22*, 1127–1137. [[CrossRef](#)]
22. Zhang, Z.H.; Yang, G.H. Distributed fault detection and isolation for multiagent systems: An interval observer approach. *IEEE Trans. Syst. Man, Cybern. Syst.* **2018**, *50*, 2220–2230. [[CrossRef](#)]

23. Li, D.; Chang, J.; Chen, W.; Raïssi, T. IPR-based distributed interval observers design for uncertain LTI systems. *ISA Trans.* **2022**, *121*, 147–155. [[CrossRef](#)] [[PubMed](#)]
24. Zhang, H.; Huang, J.; He, S. Fractional-Order Interval Observer for Multiagent Nonlinear Systems. *Fractal Fract.* **2022**, *6*, 355. [[CrossRef](#)]
25. Yu, W.; Chen, G.; Cao, M.; Kurths, J. Second-order consensus for multiagent systems with directed topologies and nonlinear dynamics. *IEEE Trans. Syst. Man Cybern. Part B (Cybern.)* **2009**, *40*, 881–891.
26. Li, Z.; Liu, X.; Fu, M.; Xie, L. Global H_∞ consensus of multi-agent systems with Lipschitz non-linear dynamics. *IET Control Theory Appl.* **2012**, *6*, 2041–2048. [[CrossRef](#)]
27. Moisan, M.; Bernard, O. Robust interval observers for global Lipschitz uncertain chaotic systems. *Syst. Control Lett.* **2010**, *59*, 687–694. [[CrossRef](#)]

Disclaimer/Publisher’s Note: The statements, opinions and data contained in all publications are solely those of the individual author(s) and contributor(s) and not of MDPI and/or the editor(s). MDPI and/or the editor(s) disclaim responsibility for any injury to people or property resulting from any ideas, methods, instructions or products referred to in the content.